Self-Organization of Multi-UAVs for Improving QoE in Unequal User Distribution

Young Jeon[1], Wonseok Lee[1], Tran Manh Hoang[2], and Taejoon kim[1,3*]
[1] Department of Information and Communication Engineering, Chungbuk National University
Cheongju 28644 Korea
[e-mail: jeony9672@chungbuk.ac.kr, ws_lee@chungbuk.ac.kr]
[2]Telecommunications University, Vietnam
[e-mail: tranmanhhoang@tcu.edu.vn]
[3] Research Institute for Computer and Information Communication, Chungbuk National University
Cheongju 28644 Korea
[e-mail: ktjcc@chungbuk.ac.kr]
[*]Corresponding author: Taejoon kim

Received November 29, 2021; revised March 8, 2022; accepted March 23, 2022; published April 30, 2022

Abstract

A self-organizing multiple unmanned aerial vehicles (multi-UAVs) deployment based on virtual forces has a difficulty in ensuring the quality-of-experience (QoE) of users because of the difference between the assumed center for users in a hotspot and an actual center for users in the hotspot. This discrepancy is aggravated in a non-uniform and mobile user distribution. To address this problem, we propose a new density based virtual force (D-VF) multi-UAVs deployment algorithm which employs a mean opinion score (MOS) as a metric of QoE. Because MOS is based on signal-to-noise ratio (SNR), a sum of users' MOS is a good metric not only to secure a wide service area but to enhance the link quality between multi-UAVs and users. The proposed algorithm improves users' QoE by combining virtual forces with a random search force for the exploration of finding multi-UAVs' positions which maximize the sum of users' MOS. In simulation results, the proposed deployment algorithm shows the convergence of the multi-UAVs into the position of maximizing MOS. Therefore, the proposed algorithm outperforms the conventional virtual force-based deployment scheme in terms of QoE for non-uniform user distribution scenarios.

Keywords: Unmanned aerial vehicle, quality-of-experience (QoE), virtual force, self-organization, mean opinion score (MOS), multi-UAVs

1. Introduction

An unmanned aerial vehicle (UAV) plays an important role in relaying data packets from users to a base station. Accordingly, for the purpose of reducing data transmission load in densely populated areas, the research on the deployment of multi-UAVs is being conducted actively [1], [2]. A UAV has a high mobility and a high probability of connecting line-of-sight (LoS) links with users [3], [4]. Hence, multi-UAVs can increase an energy efficiency and a spectrum utilization. Since a UAV has strict limitations on its communication range and battery capacity, the research for efficient multi-UAVs operation is spotlighted [5], [6]. The objectives of these researches are to cover many users within the range of multi-UAVs while maintaining the connection among the multi-UAVs [7], [8]. In [9], a circle packing approach is introduced for multi-UAVs deployment. This circle packing method aims to maximize the sum of the communication ranges of multi-UAVs. However, it is challenging to implement this method precisely because multi-UAVs have limited communication resources available. In [10], a self-organization scheme is adopted to deploy multi-UAVs in a military operational environment, where the multi-UAVs are deployed around sensors, relaying the sensors' data to a back-office. Specifically, if the connections among the multi-UAVs are maintained, the distances among the multi-UAVs are increase; however, if the connections are lost, the distances are decreased. In [11] and [12], a self-organization technique for multi-UAVs deployment based on the concept of the virtual universal gravitational force is proposed. An attraction force and a repulsion force are reflected in those proposed virtual forces, which maintain the connections among the multi-UAVs. Maintaining these connections, each UAV moves to the nearest hotspot to serve users associated with it. In [13], a mean opinion score (MOS) is introduced as a performance metric for a multi-UAVs deployment method using reinforcement learning. MOS is a representative index of quality-of-experience (QoE) and can be used to improve communication performance [14], [15].

In [11], once ground users are located around hotspots, the virtual forces are employed to deploy multi-UAVs near the hotspots. However, in an unequal user distribution, there is a discrepancy between the centers of those hotspots and the actual centers of users. Because the centers of those hotspots are the working points of the virtual forces, this discrepancy causes a misplacement of the multi-UAVs and a decrease in the users' QoE. Furthermore, when mobile users are considered, maintaining the users' QoE is an even more challenging task. To overcome the problem caused by the discrepancy between the assumed centers of users and the actual centers of users and to maintain QoE for mobile users, we propose a multi-UAVs deployment algorithm, which combines a virtual force-based deployment method with a global optimization method adopting MOS as a performance metric. The proposed scheme enhances the QoE of users when mobile and unequal user distributions are considered. In [16], a deep reinforcement learning based dynamic QoE optimization for multi-UAVs is proposed. The authors improve QoE in the viewpoint of dynamic mobile edge computing (MEC) support and an efficient data offloading for the multi-UAVs; however, the movement of the multi-UAVs is not considered. Hence, if the dynamic algorithm in [16] is combined with the proposed deployment algorithm in this paper, a further performance enhancement in supporting MEC is expected.

Because signal-to-noise ratio (SNR) is used in the calculation of MOS, if the multi-UAVs have good channel qualities in the links connected with users on densely populated areas, those users will have very high MOS values. Consequently, when the multi-UAVs approach their actual center of users, the sum of those users' MOS increases. In a mobile users' scenario, it is difficult to determine the optimal position of the multi-UAVs guaranteeing the

communication performance of the mobile users [17]. However, if the multi-UAVs move to the position where the sum of users' MOS achieves the highest value, that position will be closer to the centers of users' clusters, and the high communication performance will be attained. To maximize users' MOS, the proposed algorithm includes a random force to prevent multi-UAVs from being stuck to a local optimal point. In addition, while keeping the links among the multi-UAVs being connected, the random search force combined with the other virtual forces searches for positions where the sum of users' MOS can be maximized. In order to adopt the concept of the simulated annealing, as the searching round goes on, the random search force is gradually reduced, and a virtual force of leading the multi-UAVs to the optimal position, which is guaranteed to be so far best, gradually increases.

In the literature, there are two different strategies in deploying multi-UAVs. One of them is to maximize the number of links between multi-UAVs and users while guaranteeing a minimum link quality [10], [11], and [12]. The other is to maximize the total throughput of a considered network [13] and [18]. The strategy of maximizing the number of links has a weakness in enhancing the links between the multi-UAVs and the users. To the contrary, the strategy of maximizing total throughput may neglect some isolated users resulting in a reduced service area. However, the proposed deployment algorithm strikes a good trade-off between the link maximization strategy and the throughput maximization strategy. Specifically, at initial phase, the proposed algorithm quickly spread the multi-UAVs over a wide area through a gravitational virtual force-based deployment scheme. Afterwards, the link quality is enhanced through a global search-based MOS maximization. This combined process shows an excellent performance both in increasing the number of link and in enhancing the quality of the links. To the best of our knowledge, this algorithm is novel and innovative. In addition, a thorough simulation study shows that the proposed algorithm, under various unequal user distribution, successfully finds the optimal multi-UAVs position where the QoE of users is maximized. Moreover, the results of the simulation study confirms that the proposed algorithm outperforms the conventional virtual force-based algorithm under various scenarios.

The remainder of this paper is organized as follows: Section 2 describes a system model, Section 3 introduces the procedure of the proposed algorithm, and Section 4 compares the performances of the proposed algorithm with the conventional virtual force-based algorithm in both static and mobile environments. Section 5 concludes the paper.

2. System Model

2.1. Channel model

An air-to-ground (ATG) model is adopted between a UAV and a user equipment (UE) [19]. A set of UAVs and a set of UEs are defined as $\mathcal{K} = \{1, 2, \cdots, K\}$ and $\mathcal{N} = \{1, 2, \cdots, N\}$, respectively. The ATG model considers a probability of establishing a LoS link and a non-LoS (NLoS) link between a UAV and a UE [20]. The following is a LoS probability between kth UAV and nth UE.

$$P\left(LoS, \theta_{k,n}\right) = \frac{1}{1 + \alpha \exp\left(-\beta\left(\theta_{k,n} - \alpha\right)\right)}, \tag{1}$$

where α and β are constants affected by an environment, $\theta_{k,n}$ is the elevation angle formed by kth UAV and nth UE. $P\left(NLoS, \theta_{k,n}\right) = 1 - P\left(LoS, \theta_{k,n}\right)$ is satisfied, and the following

is an average path loss formula considering both the LoS and the NLoS links.

$$PL = P(\mathrm{LoS}, \theta_{k,n}) \cdot L_{\mathrm{LoS}} + P(\mathrm{NLoS}, \theta_{k,n}) \cdot L_{\mathrm{NLoS}}\,, \tag{2}$$

where L_{LoS} and L_{NLoS} are path loss for LoS and NLoS, respectively, and they are given by

$$L_{LoS} = 20\log\left(\frac{4\pi f_{\mathrm{c}}}{c}\right) + \eta_{\mathrm{LoS}}\,, \tag{3}$$

$$L_{NLoS} = 20\log\left(\frac{4\pi f_{\mathrm{c}}}{c}\right) + \eta_{\mathrm{NLoS}}\,, \tag{4}$$

where f_c is the center frequency and c is the speed of light. L_{LoS} and L_{NLoS} are calculated by adding an environment-dependent additional path loss to a free space propagation loss (FSPL). For convenience of calculation, additional path losses are averaged and denoted in η_{LoS} and η_{NLoS} [21]. The following is an overall path loss equation.

$$\begin{aligned} PL_{(k,n)}(h_k, d'_{k,n}) &= 20\log\left(\frac{4\pi f_{\mathrm{c}}}{c}\right) + 20\log\left(\sqrt{h_k^2 + {d'_{k,n}}^2}\right) + P(LoS, \theta_{k,n}) \cdot \eta_{\mathrm{LoS}} \\ &\quad + P(NLoS, \theta_{k,n}) \cdot \eta_{\mathrm{NLoS}}\,, \end{aligned} \tag{5}$$

where h_k is the altitude of kth UAV, $d'_{k,n}$ is the horizontal distance between kth UAV and nth UE.

2.2. Virtual force

In [11], a virtual force is made up of an attractive force and a repulsive force. The attractive force between UAV k_1 and UAV k_2 is calculated as follows:

$$\overrightarrow{F_{k_1,k_2}} = \overrightarrow{K_{k_1,k_2} \times \frac{1}{\left(d_{k_1,k_2}\right)^2}}\,, d_{k_1k_2} < R_{\mathrm{c}}, \tag{6}$$

where K_{k_1,k_2} is an attractive force factor, d_{k_1,k_2} is the distance between UAV k_1 and UAV k_2, and R_{c} is the communication range of the UAVs. The repulsive force is calculated as follows:

$$\overrightarrow{f_{\mathrm{a}}} = \overrightarrow{K_{\mathrm{r}} \times (R_{\mathrm{opt}} - d_{k_1,k_2})}\,, d_{k_1,k_2} < R_{\mathrm{opt}}, \tag{7}$$

where K_{r} is a repulsive force factor and R_{opt} is a minimum distance to prevent collisions with neighboring UAVs.

2.3. Quality-of-experience model

In [14], MOS is a metric for evaluating the QoE of users, and the calculation of MOS for sender i and receiver j is as follows:

$$MOS_{ij}(t) = -K_1 \ln\big(d(r_i)\big) + K_2 \,, \tag{8}$$

where $d(r_i)$ is a delay time when a sender i transfers data to a receiver j at a data rate of r_i. K_1 and K_2 are constants for calculating MOS.

3. D-VF Algorithm

A density based virtual force (D-VF) algorithm newly is proposed, which deploys the multi-UAVs based on virtual forces with considering MOS. In [11], the virtual forces are used to locate multi-UAVs around hotspots and to maintain connections among the multi-UAVs. However, if UEs are not distributed uniformly around the hotspots, the communication link quality between the multi-UAVs and UEs will be severely deteriorated.

As shown in **Fig. 1**, there are three major examples of non-uniform UE distributions around a hotspot. The blue points represent UEs, and a black point is a center point of the hotspot presumed by the virtual force method, and red triangles are the actual centers of the UEs. **Fig. 1(a)** depicts that UEs are distributed unequally in a direction from the center of the hotspot to the right. In this case, the actual center of UEs and the center of the hotspot do not match, which results in the performance degradation. **Fig. 1(b)** depicts a scenario in which UEs spread horizontally around the center of a hotspot. In this case, although the actual center of UEs is close to the assumed center of the hotspot, it is desirable to split the UEs into small groups of two. Moreover, after splitting the UEs into two small groups, adding one more UAV is suggested as a better option. **Fig. 1(c)** depicts a situation in which many UEs are crowded around a hotspot. In this case, the assumed center of the hotspot and the center of UEs are very close to each other. However, more than a single UAV need to be deployed to support the numerous connections between the UAV and the UEs. When UEs are unequally crowded, D-VF, which uses MOS metric, improves the quality of communication with UEs in hotspots.

As the multi-UAVs approach their actual center of the UEs, the sum of the UEs' MOS increases. For the multi-UAVs, pursuing the position achieving the highest total-MOS can reduce the discrepancy between the assumed centers of hotspots and the actual centers of UEs. For the deployment of the multi-UAVs, a maximization of the total-MOS and an exploration of a random searching for better position are introduced in [22]–[24]. In D-VF, local MOS and global MOS are newly introduced to maximize the coverage of the multi-UAVs and the total-MOS of UEs. The local MOS of UAV k in round t is denoted as $L^k(t)$, which is a best so far local sum of MOSs for the UEs connected to UAV k up to round t [25], and it is given by

$$L^k(t) = \max\left(L^k(t-1), \sum_{n \in \mathcal{N}_k} MOS_{(k,n)}(t)\right), \tag{9}$$

where $\mathcal{N}_k$ is the set of UEs connected to the UAV k, $MOS_{(k,n)}(t)$ is the MOS of UE n connected to UAV k in round t. To converge the position of UAV k to the optimal position where the local MOS is maximized, the UAV k should save the coordinate of the optimal position. The universal gravitational force of local MOS from the saved position is as follows:

$$\overrightarrow{F_{\mathrm{LM}}} = \overrightarrow{K_{\mathrm{LM}} \times \frac{1}{{d_{\mathrm{LM}}}^2}}, \tag{10}$$

where K_{LM} is the local MOS factor whose value is listed in **Table 1**, d_{LM} is the distance between a UAV and the saved position, and $\overrightarrow{F_{\mathrm{LM}}}$ is an attractive force into the saved position. The global MOS is denoted as $G(t)$, which is a best so far sum of MOSs of all the UEs connected with any UAV in round t, and it is given by

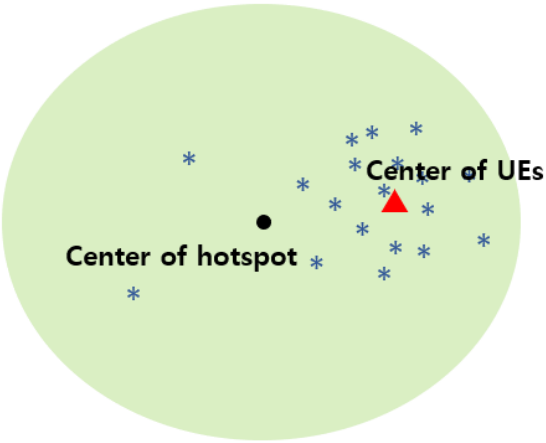

(a) Unequal UE deployment in hotspot

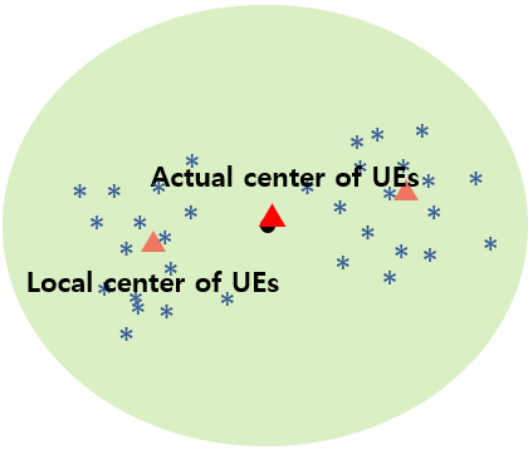

(b) UE deployment divided into two hotspots

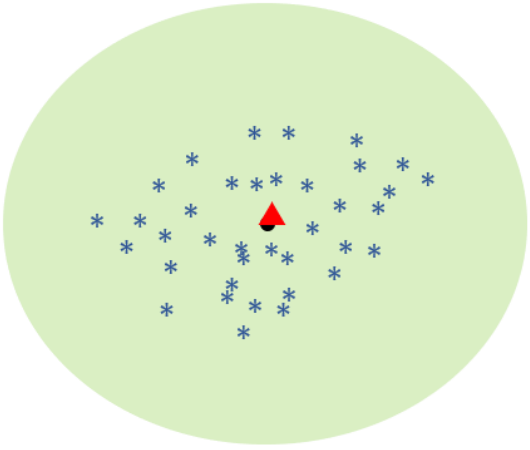

(c) Multiple UE deployment in hotspot

Fig. 1. Exemplary UE deployments in a hotspot.

$$G(t) = \max\left(G(t-1), \sum_{k \in \mathcal{K}} \sum_{n \in \mathcal{N}_k} MOS_{(k,n)}(t) \right). \tag{11}$$

Then, each UAV stores the coordinate of the multi-UAVs that maximize the global MOS. The universal gravitational force of global MOS from the saved positions is as follows:

$$\overrightarrow{F_{\mathrm{GM}}} = \overrightarrow{K_{\mathrm{GM}} \times \frac{1}{{d_{\mathrm{GM}}}^2}}, \tag{12}$$

where K_{GM} is the global MOS factor whose value is shown in **Table 1**, and d_{GM} is the distance between a UAV and the coordinate stored in the UAV. An exploration algorithm of the multi-UAVs deployment uses a random search virtual force to avoid falling into a local optimal point. The random search virtual force is shown as follows:

$$\overrightarrow{F_{\mathrm{R}}} = \overrightarrow{k_{\mathrm{r}} \times R_k}, \tag{13}$$

where k_{r} is a random search force factor whose value is shown in **Table 1**, and R_k is a two-dimensional random vector with a unit size for UAV k. To adjust the ratio between exploration and optimization, the magnitude of the random search virtual force can be changed. By summing up all the virtual forces of inter-UAVs (attraction plus repulsion), local MOS, global MOS, and random search, the total force $\overrightarrow{F_k}$ is applied to UAV k as follows:

$$\overrightarrow{F_k} = \alpha(t) \cdot \left(\overrightarrow{F_{k_1,k_2}} + \overrightarrow{f_a} \right) + \beta(t) \cdot \overrightarrow{F_{\mathrm{LM}}} + \gamma(t) \cdot \overrightarrow{F_{\mathrm{GM}}} + \zeta(t) \cdot \overrightarrow{F_{\mathrm{R}}}, \tag{14}$$

where $\alpha(t)$, $\beta(t)$, $\gamma(t)$, and $\zeta(t)$ are adjustment parameters for the virtual forces of inter-UAVs, local MOS, global MOS, and random search, respectively. The formulas for these adjustment parameters are as follows:

$$\alpha(t) = \exp\left(-p \cdot (t - \tau_1)\right), t > \tau_1, \tag{15}$$

$$\beta(t) = \exp\left(-p \cdot (t - \tau_2)\right), t > \tau_2, \tag{16}$$

$$\gamma(t) = 1 - \exp\left(-p \cdot (t - \tau_3)\right), t > \tau_3, \tag{17}$$

$$\zeta(t) = \exp\left(-p \cdot (t - \tau_4)\right), t > \tau_4, \tag{18}$$

where p is an exponent for the diminishing virtual forces as the round goes, i.e., the virtual forces for inter-UAVs, local MOS, and random search. If p is high, these virtual forces diminish more quickly, while the virtual force for global MOS increases sharply as the round goes. τ_1, τ_2, τ_4 are the time epochs when these three virtual forces (inter-UAVs, local MOS, and the random search) start to diminish, and τ_3 is the time epoch when the global MOS virtual force start to increase. Because $\overrightarrow{F_k}$ can be increased from 0 to +∞, mapping to a finite value is required. Let $\overrightarrow{F_k}$ map to a value between 0 and V_k, where V_k is a maximum velocity of UAV k, and this mapping is implemented using $\arctan()$ as follows:

$$v_k = \arctan\left(\overrightarrow{F_k}\right) \cdot \frac{2}{\pi} \cdot V_k. \tag{19}$$

Hence, at each round, the UAV k moves at a speed of v_k to the direction of $\overrightarrow{F_k}$. The following is the process of D-VF algorithm for the multi-UAVs deployment, and this process is summarized in Algorithm 1.

1. Multi-UAVs are randomly placed in a region of interest.

2. At every round, the attractive virtual force and the repulsive virtual force are re-calculated with the current multi-UAVs position.

3. For each UAV, the local MOS of UEs with the current UAV position is calculated. And it updates the local MOS information if the current local MOS is higher than the stored local MOS.

4. Update the global MOS of overall UEs if the current round global MOS is higher than the stored global MOS. When $t > \tau_1, \cdots, t > \tau_4$, the associated virtual forces start to be adjusted.

5. For each UAV, all the virtual forces are calculated aggregated, and the aggregated total virtual force is applied to the UAV.

6. Advance to the next round by going to step 2.

Algorithm 1. D-VF multi-UAVs deployment algorithm

Input:

$\mathcal{K}$, $\mathcal{N}$, R_{opt}, K_{k_1,k_2}, $K_{\mathrm{r}}, R_{k_1}, K_{\mathrm{LM}}$, K_{GM}, k_{r}, τ_1, τ_2, τ_3, τ_4, T, $\mathcal{K}_0^{pos}$, V_{k_1}, R_c

Output:

$\mathcal{K}_T^{pos}$ for UAV i, MOS_j, Throughput for $1 \le i \le |\mathcal{K}|$, $1 \le j \le |\mathcal{N}|$

for each $t < T$
  for each $k_1 \in \mathcal{K}$
    for each $k_2 \in \mathcal{K}, k_2 \neq k_1$
      if $d_{k_1 k_2} < R_c$
        $\overrightarrow{F_{k_1,k_2}} = \overrightarrow{K_{k_1,k_2} \times \frac{1}{(d_{k_1,k_2})^2}}$
      end if
      if $d_{k_1 k_2} < R_{\mathrm{opt}}$

8: $\overrightarrow{f_{\mathrm{a}}} = K_{\mathrm{r}} \times \left(R_{\mathrm{opt}} - d_{k_1,k_2}\right)$

9: **end if**

10: **end for**

11: **for each** $n \in \mathcal{N}$

12: $MOS_{(k_1,n)}(t) = -K_1 \ln\left(d\left(r_{k_1}\right)\right) + K_2$ eqn. (8)

13: **end for**

14: $L^{k_1}(t) = \max\left(L^{k_1}(t-1), \sum_{n\in\mathcal{N}_{k_1}} MOS_{(k_1,n)}(t)\right)$ eqn. (9)

15: **if** $L^{k_1}(t) \geq L^{k_1}(t-1)$

16: position update d_{LM}

17: **end if**

18: **end for**

19: $G(t) = \max\left(G(t-1), \sum_{k_1\in\mathcal{K}} \sum_{n\in\mathcal{N}_{k_1}} MOS_{(k_1,n)}(t)\right)$ eqn. (11)

20: **if** $G(t) \geq G(t-1)$

21: position update d_{GM}

22: **end if**

23: $\overrightarrow{F_{\mathrm{LM}}} = \overrightarrow{K_{\mathrm{LM}} \times \frac{1}{{d_{\mathrm{LM}}}^2}}, \overrightarrow{F_{\mathrm{GM}}} = \overrightarrow{K_{\mathrm{GM}} \times \frac{1}{{d_{\mathrm{GM}}}^2}}, \overrightarrow{F_{\mathrm{R}}} = \overrightarrow{k_{\mathrm{r}} \times R_{k_1}}$ eqns. (10), (12), and (13)

24: **for each** $k_2 \in \mathcal{K}, k_1 \neq k_2$

25: $\overrightarrow{F_{k_1}} = \alpha(t) \cdot \left(\overrightarrow{F_{k_1,k_2}} + \overrightarrow{f_a}\right) + \beta(t) \cdot \overrightarrow{F_{\mathrm{LM}}} + \gamma(t) \cdot \overrightarrow{F_{\mathrm{GM}}} + \zeta(t) \cdot \overrightarrow{F_{\mathrm{R}}}$ eqn. (14)

26: **end for**

27: $v_{k_1} = \arctan\left(\overrightarrow{F_{k_1}}\right) \cdot \frac{2}{\pi} \cdot V_{k_1}$

28: **end for**

In Algorithm 1, $\mathcal{K}_t^{pos}, t = 0, \cdots, T$ is the multi-UAVs' position in round t, and $\mathcal{K}_T^{pos}$ is the optimal position. In line 11-13 of Algorithm 1, the MOS of UEs is calculated considering the set of UEs $\mathcal{N}$ and the set of UAVs $\mathcal{K}$ over all the rounds. Therefore, the complexity of D-VF algorithm is $O(|\mathcal{K}||\mathcal{N}|T)$, and $|\cdot|$ is a cardinality of a set. The D-VF algorithm searches for densely populated areas and optimizes the deployment of the multi-UAVs quickly. Consequently, the QoE of the UEs is enhanced, resulting in the improved communication quality.

4. Simulation Results

4.1. Simulation setup

A multi-UAV simulator built with Java is used to compare the performances of D-VF with conventional virtual force (VF) algorithm [26]. The performance metrics for the simulation are the number of links between the multi-UAVs and the UEs, average-MOS of all the UEs, and moving fairness [16]. The size of an area of interest is 2000 m × 2000 m. The simulation parameters are shown in **Table 1**.

Table 1. Simulation parameters

Parameters	Value
UAV altitude, h_{uav}	100 m
communication range of UAV, R_c	400 m
number of covered UEs in UAV	20
attraction force factor, K_{k_1,k_2}	5500
repulsive force factor, K_{r}	3500
local MOS force factor, K_{LM}	500
global MOS force factor, K_{GM}	700
random force factor, k_{r}	10
LoS, η_{LoS}	1 dB
NLoS, η_{NLoS}	20 dB
SINR threshold	-7 dB
random walk speed	1 m/s
maximum speed of UAV, V_k	10 m/s
range of hotspot	300 m

In this simulation, L_{N} is denoted as the number of connected links between the multi-UAVs and the UEs.

4.2 Performance analysis with static hotspots

As shown in **Fig. 2**, the UEs (red point) are placed around the hotspots (blue point) and the multi-UAVs (black circle) are placed across the area. The UEs are located within the range of the hotspot (yellow circle). For the purpose of validating the performance of D-VF under various UE distributions, the simulation is conducted over six different randomly generated distributions shown in **Fig. 2**.

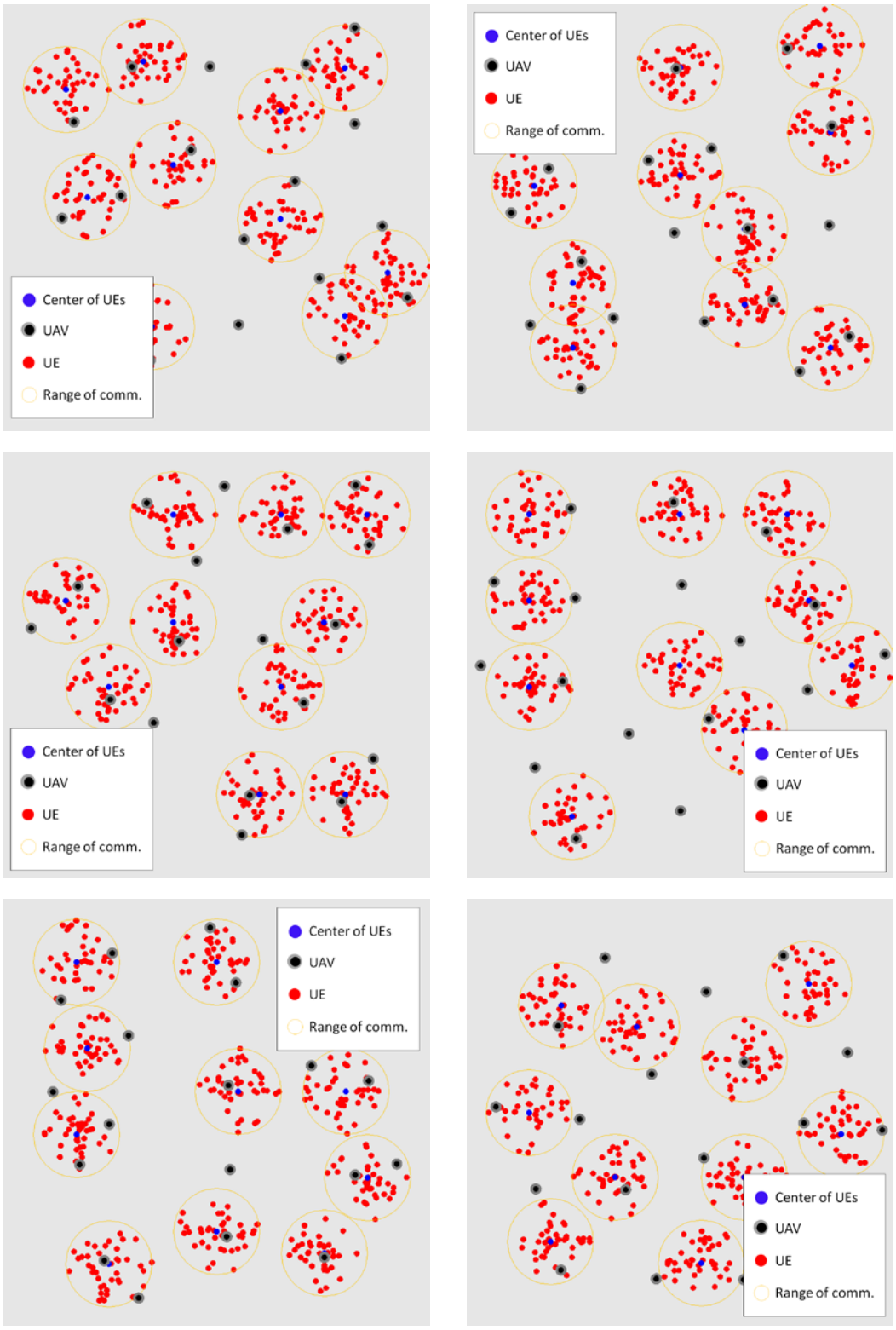

Fig. 2. Multi-UAVs and static UEs deployments around hotspots with six distributions.

In **Fig. 3**, L_Ns with VF and D-VF with six distributions are depicted. On average after 200 rounds, L_N with D-VF becomes stable. However, VF has fluctuations over long period. Note that since VF considers only attractive and repulsive factors for the virtual forces, it may suffer from oscillation even when the position of the multi-UAVS is close to the balancing point between the attractive force and the repulsive force. To the contrary, D-VF reduces the attractive virtual force and the repulsive virtual force at later rounds, and the global MOS virtual force quickly stabilize the position of the multi-UAVs by moving the multi-UAVs to the best so far highest MOS position. The multi-UAVs with VF have connections of 278, 272,

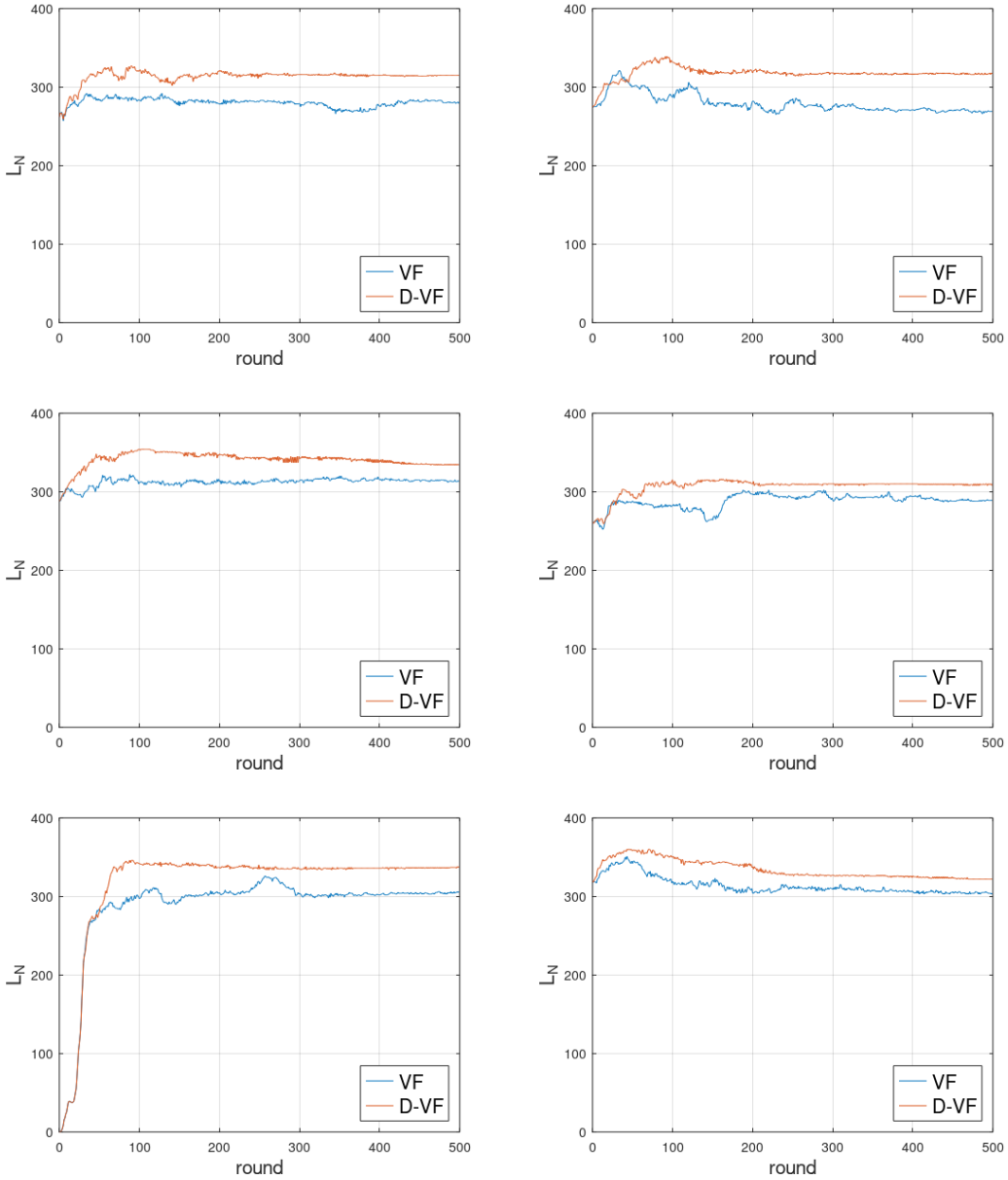

Fig. 3. The number of connected links by VF and D-VF with six distributions.

314, 292, 305, 307 from subplot (1st row, 1st column) to (3rd row, 2nd column), whereas the multi-UAVs in D-VF have connections of 315, 317, 340, 309, 336, 326. Hence, D-VF has on average 29 more connections and lower fluctuations in L_{N} than VF.

In **Fig. 4**, the average-MOSs for VF, D-VF, and theoretical maximum MOS are depicted. To measure the theoretical maximum MOS, a single UAV and 20 UEs are deployed at a common horizontal position, and the measured value is 3.39. Note that, a UAV can serve the maximum 20 UEs in this simulation setting. Similar to **Fig. 3**, VF has more fluctuations compared to D-VF. Moreover, for VF the improvement of the average-MOS is marginal as the round goes on. To the contrary, the average-MOS of D-VF gradually increases roughly util 200 rounds or

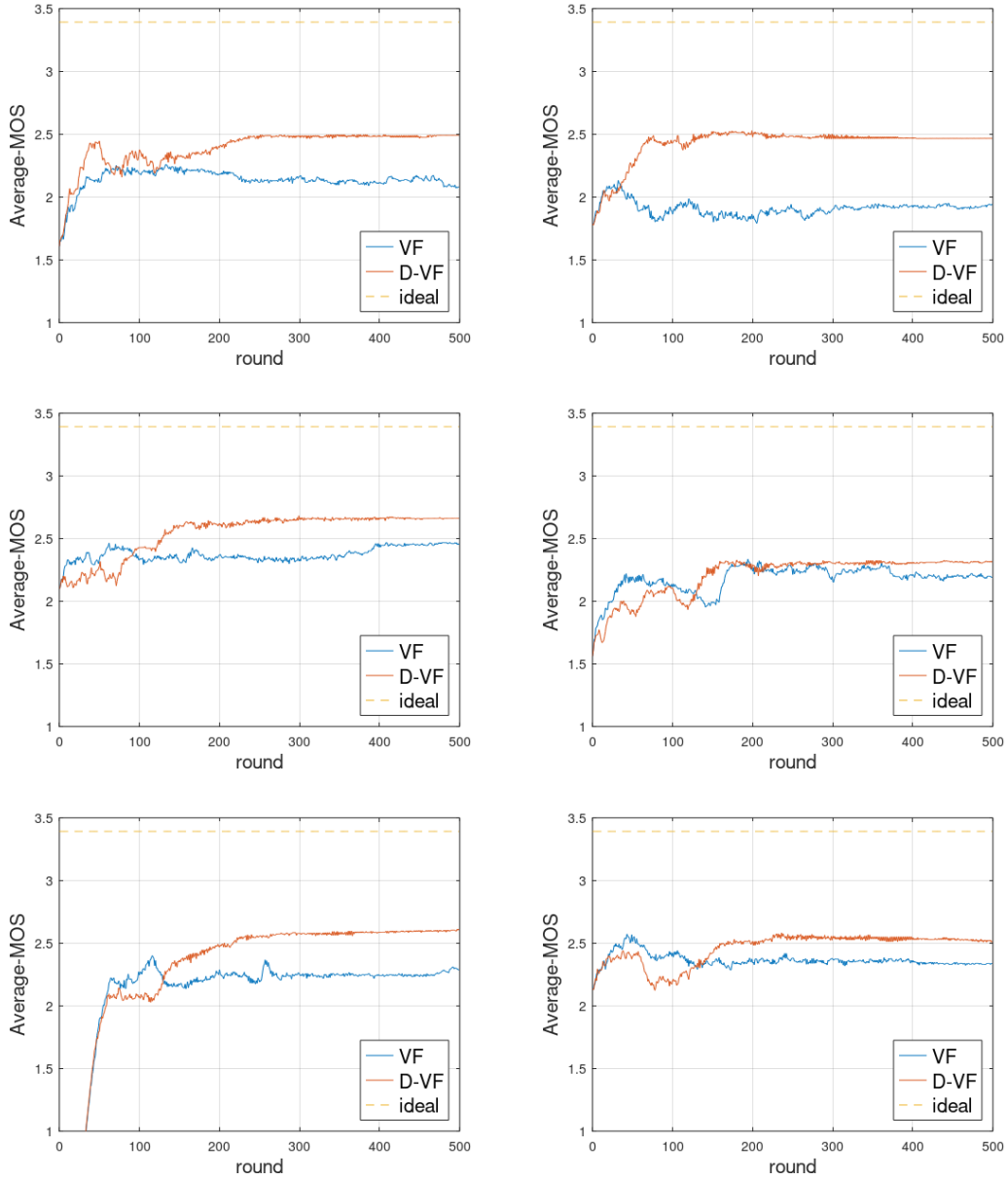

Fig. 4. Average-MOS of VF and D-VF with six distributions.

more. The average-MOS of VF converges to 2.13, 1.9, 2.38, 2.22, 2.24, 2.35 in each distribution, while the average-MOS of D-VF converges to 2.47, 2.47, 2.64, 2.3, 2.57, 2.53. The results show that D-VF has on average 13% higher average-MOS than VF. As we can see in **Fig. 3 - Fig. 4**, for the static UE scenarios, D-VF outperforms VF in terms of QoE and connectivity with UEs.

4.3 Performance analysis with varying numbers of multi-UAVs

With the first UEs distribution shown in **Fig. 2**, L_N, average-MOS, and moving fairness of D-VF are compared with those of VF when the number of the multi-UAVs increases.
In **Fig. 5**, L_{N} with the increasing number of the multi-UAVs is shown, and as shown in this figure, the multi-UAVs deployed with D-VF are connected to more UEs than the multi-UAVs deployed with VF. It means that regardless of the number of the multi-UAVs, D-VF more effectively covers the service area and successfully establish connections with UEs. Specifically, L_{N} with D-VF exceeds L_{N} with VF by 19.2%, 17%, 13.3%, 10.2%, and 16.8% when the number of the multi-UAVs ranges from 14 to 22 with a step size two.

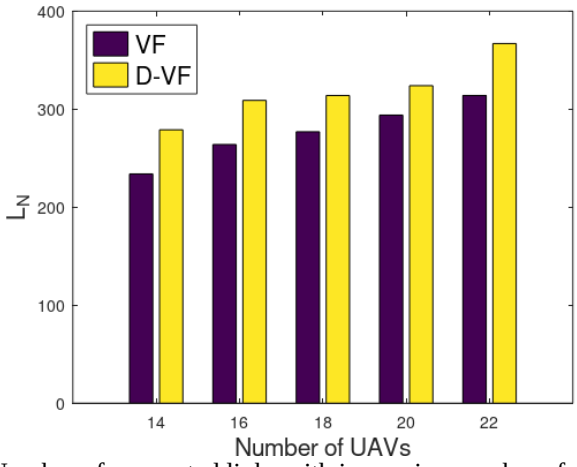

Fig. 5. Number of connected links with increasing number of multi-UAVs.

In **Fig. 6**, the average-MOSs for D-VF, VF, and theoretical maximum are depicted when the number of the multi-UAVs increases from 14 to 22. When the number of the multi-UAVs is 14. The gap between VF and D-VF is small; however, the gap increases as the number of the multi-UAVs further increases. When the number of the multi-UAVs is small, both D-VF and VF have a difficulty in finding a better deployment because the connections among the multi-UAVs should be maintained. Accordingly, it is quite natural that the gap between VF and D-VF is small in this case. However, as the number of the multi-UAVs increases, the multi-UAV can build various formations. Hence, D-VF can actively search the optimal multi-UAVs position. D-VF has 3.1%, 16.01%, 16.98%, 14.03%, and 20.08% higher average-MOS than VF. As a result, the multi-UAVs with D-VF maintain more links and have a higher QoE than the multi-UAVs with VF. As we can see in **Fig. 5 - Fig. 6**, D-VF outperforms VF in terms of link establishment and QoE enhancement when the number of UAVs is increased.
During the multi-UAVs deployment phase, it is desirable that the total moving distance of each UAV being similar with each other, which is referred to as moving fairness. Then, Jains' fairness index is used in [11] formulating this moving fairness as follows:

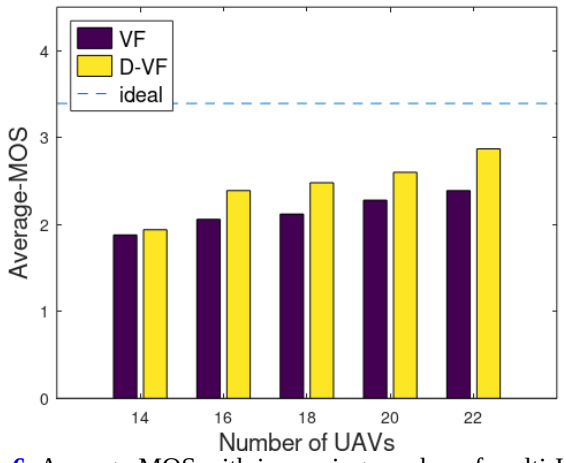

Fig. 6. Average-MOS with increasing number of multi-UAVs.

$$\psi_{\mathrm{m}} = \frac{\left(\sum_{k=1}^{|\mathcal{K}|} D_{\mathrm{m}}^{k}\right)^{2}}{|\mathcal{K}| \cdot \sum_{k=1}^{|\mathcal{K}|} \left(D_{\mathrm{m}}^{k}\right)^{2}}, \tag{20}$$

where D_{m}^{k} is the moving distance of UAV k, and $|\mathcal{K}|$ is the total number of the multi-UAVs. The comparison of the moving fairness between VF and D-VF is shown in **Fig. 7**. In this figure, the multi-UAVs in D-VF have the less disparity of moving distances than the multi-UAVs in VF. In the case of VF, the moving fairness largely decreases as the number of the multi-UAVs increases. It means that VF cannot properly utilize the extra UAVs when the number of the multi-UAVs increases. Accordingly, there may be a hazardous situation that some UAVs are over-utilized while the remaining UAVs are under-utilized in the deployment process. Because of those over-utilized UAVs, an operation of the multi-UAVs can be terminated earlier than expected. In contrast, in the case of D-VF, even when the number of the multi-UAVs increases, the moving fairness remains nearly constant. It means that D-VF utilizes the multi-UAVs more evenly than VF. Therefore, D-VF has an advantage in extending the lifetime of the considered UAV network.

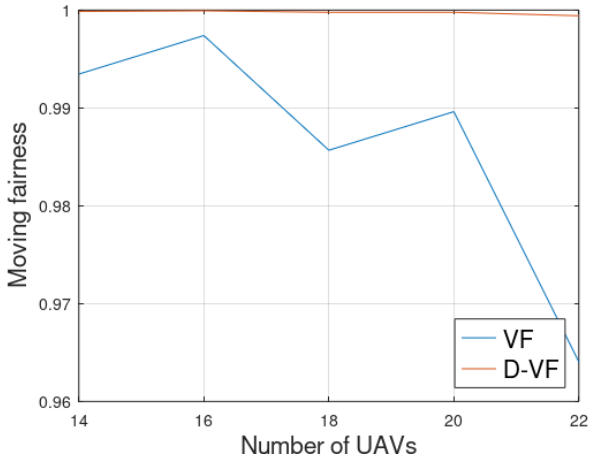

Fig. 7. Moving fairness of VF and D-VF.

Fig. 8 shows the MOS distribution with the static UEs distribution given in **Fig. 2**. When the MOS of a spot is high, the color of that spot is close to dark red, and if it is low, the color of that spot is close to dark blue. The assumed center point of a hotspot is marked as a green triangle, and the UEs are marked as white points. When the center of the hotspot and a densely populated area of the UEs do not coincide, the position of multi-UAVs need to be adjusted toward the populated area of the UEs.

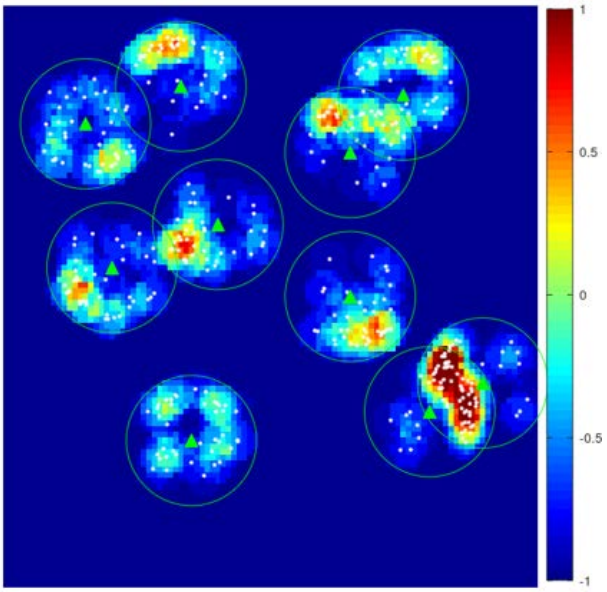

Fig. 8. MOS distribution with UEs in **Fig. 2**.

4.4 Performance analysis with moving UEs

In VF, each UAV moves to the assumed center of the closest hotspot and covers the UEs associated with the hotspot. If the hotspot moves, the UEs will move along with the hotspot. Accordingly, when the hotspot and the UEs move, there is a gap between the actual center of the UEs and the assumed center of the hotspot. D-VF is based on the measured MOS of UEs and presents a good solution for this kind of moving UEs scenarios.

In **Fig. 9 - Fig. 10**, the simulation results show L_N and average-MOS with moving UEs scenarios. In these figures, both the hotspots and the associated UEs move in a random walk fashion while the UEs' random walk is regulated not to cross the range of the hotspots. The hotspots and the UEs move at the speed of 1 m/round. In these figures, both L_N and the average-MOS increase sharply at early rounds whether the adopted algorithm is VF or D-VF. It means that, compared to the static scenarios, the attractive and the repulsive virtual forces play an important role at early rounds. Because the UEs moves continuously, it takes longer rounds in stabilizing the deployment based on the attractive and the repulsive virtual forces. However, D-VF extracts more gain in both L_N and average-MOS by further optimizing the multi-UAVs position. In **Fig. 9**, the average L_Ns for VF and D-VF are 277 and 295, respectively. D-VF has more connections with UEs than VF. **Fig. 10** shows the average-MOS with moving hotspots and moving UEs. The average-MOS of VF is 2.16, whereas the average-MOS of D-VF is 2.39. As the multi-UAVs with D-VF approach the center of the UEs, the average-MOS increases. D-VF follows the actual center of the UEs more closely than VF. As we can see in **Fig. 9 - Fig. 10**, D-VF has better performances than VF in terms of link establishment and QoE enhancement when the hotspot and the UEs move randomly.

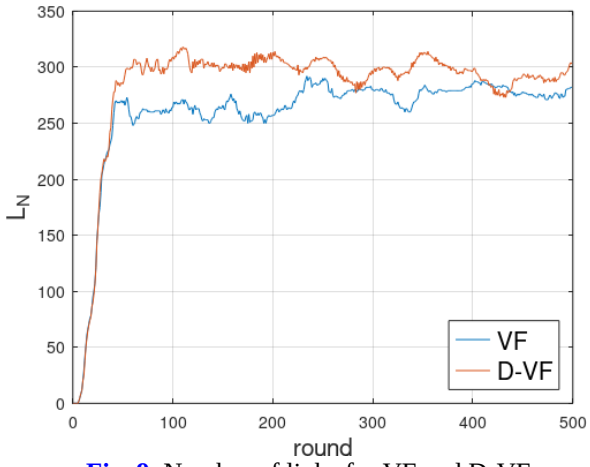

Fig. 9. Number of links for VF and D-VF.

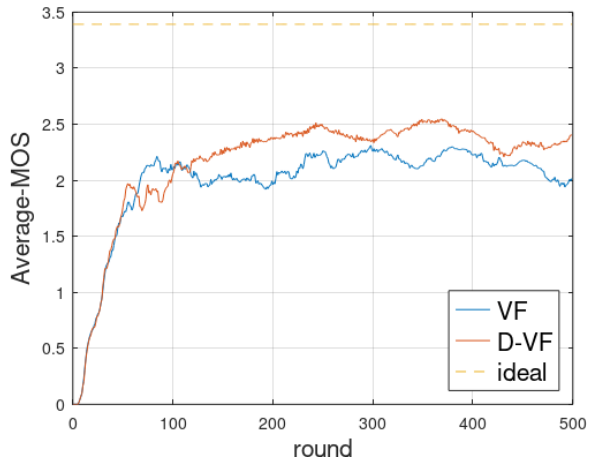

Fig. 10. Average-MOS for VF and D-VF.

In **Fig. 11 - Fig. 12**, the hotspots move to the right and the associated UEs move randomly around the moving hotspots. **Fig. 11** shows L_N between the multi-UAVs and the UEs. **Fig. 11 - Fig. 12** are largely similar with **Fig. 9 - Fig. 10**, because the UEs moves continuously. Hence, the attractive and the repulsive virtual forces play an important role at early rounds. Compared to the static case, even D-VF has fluctuations because the distribution of the UEs keeps changing. The average L_Ns of VF and D-VF are 260 and 280, respectively. **Fig. 12** shows the average-MOS for this moving UEs scenario. The average-MOSs of VF and D-VF are 1.9 and 2.09, respectively. Compared to VF, D-VF establishes more connections between the multi-UAVs and the UEs and obtains high average-MOS for the UEs.

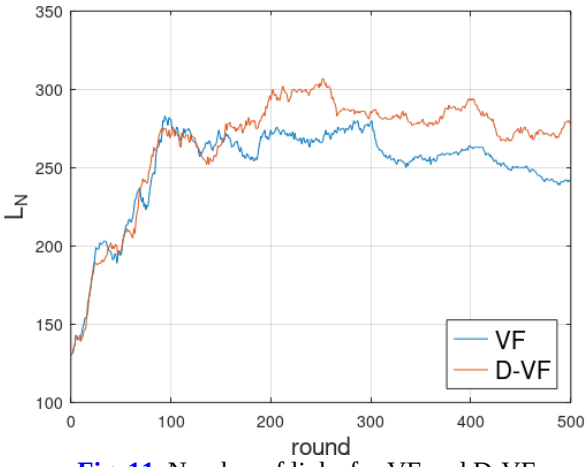

Fig. 11. Number of links for VF and D-VF.

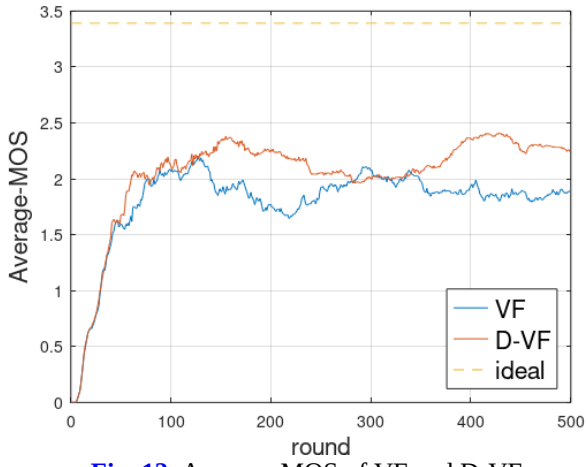

Fig. 12. Average-MOS of VF and D-VF.

In **Fig. 13 - Fig. 14**, eighteen UAVs and all the associated UEs are location at a single point. Then, as the round goes, the UEs move to predetermined positions forming seven hotspots. Once the locations of the hotspots are fixed, the UEs move randomly around the hotspot. **Fig. 13** shows L_N between the multi-UAVs and the UEs. Compared to the previous two mobile scenarios, it has more fluctuation at its early rounds. Note that, in this scenario, many UEs come together at early rounds. Accordingly, a small displacement of the multi-UAVs causes the large change of UEs connection, and it results in more fluctuations at early rounds. Moreover, this mobile UEs scenario shows the largest performance gap between VF and D-VF. In this case, compared to the previous two mobile scenarios, the distances among the hotspots largely change. Accordingly, the result suggests that D-VF more actively adapt to the change of the distances among the hotspots. The average L_Ns of VF and D-VF are 180 and 249, respectively. **Fig.14** shows the average-MOS for this moving UEs scenario. The average-MOSs for VF and D-VF are 2.12 and 2.85, respectively. Compared to VF, D-VF establishes more connections between the multi-UAVs and the UEs and obtains high average-MOS for the UEs.

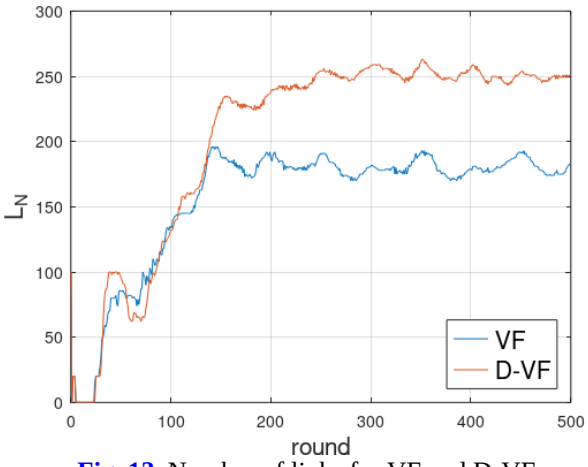

Fig. 13. Number of links for VF and D-VF.

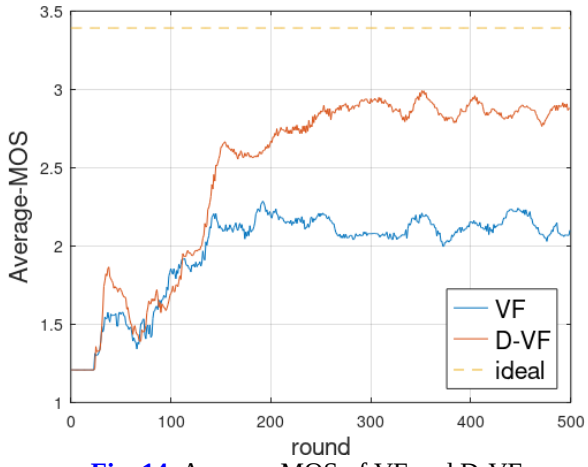

Fig. 14. Average-MOS of VF and D-VF.

5. Conclusion

It is known that VF shows good performance in establishing the links between multi-UAVs and UEs. However, when the UEs in a network are unequally distributed, QoE is significantly degraded. We presented D-VF algorithm which adopts MOS to improve QoE. D-VF combines VF with MOS based virtual forces to improve the QoE of the UEs while keeping the links among the multi-UAVs being connected. When the UEs are stationary, the multi-UAVs move to densely populated areas of the UEs to increase the connectivity and the QoE of the UEs. Also, even if the UEs move, the multi-UAVs can maintain connections to the moving UEs. The simulation results show the increased connectivity with UEs, resulting in the increased average-MOS. The increase of average-MOS also indicates an improvement of QoE. Even when the UEs move randomly around hotspot areas, D-VF achieves higher QoE and connectivity of the UEs than VF. The limitations of D-VF can be considered in two aspects. The first one is that the convergence time of D-VF is affected by the initial distribution of the multi-UAVs because the virtual forces among the UAVs are dependent on the initial

distribution of the multi-UAVs. The second one is that D-VF needs to be updated frequently when the UEs move fast. Accordingly, the accuracy of D-VF can be reduced when D-VF update interval is shorter than the D-VF's convergence time. Therefore, a robust multi-UAVs deployment under fast moving UEs environment will be an interesting future research topic.

Acknowledgement

This research was supported from Chungbuk National University BK (Brain Korea) 21 FOUR (2021) and the Basic Science Research Program through the National Research Foundation of Korea (NRF) funded by the Ministry of Education under Grant 2020R1I1A3068305.

References

[1] L. Gupta, R. Jain, and G. Vaszkun, "Survey of Important Issues in UAV Communication Networks," *IEEE Communications Surveys & Tutorials*, vol. 18, no. 2, pp. 1123-1152, Secondquarter 2016. Article (CrossRef Link)

[2] Fu Xiaowei and Gao Xiaoguang, "Multi-UAVs cooperative control in communication relay," in *Proc. of 2016 IEEE International Conference on Signal Processing, Communications and Computing (ICSPCC)*, pp. 1-5, 2016. Article (CrossRef Link)

[3] A. Al-Hourani, S. Kandeepan, and S. Lardner, "Optimal LAP Altitude for Maximum Coverage," *IEEE Wireless Communications Letters*, vol. 3, no. 6, pp. 569-572, Dec. 2014. Article (CrossRef Link)

[4] Zhao, Taifei, et al., "The Coverage Method of Unmanned Aerial Vehicle Mounted Base Station Sensor Network Based on Relative Distance," *International Journal of Distributed Sensor Networks*, vol. 16, no. 5, May. 2020. Article (CrossRef Link)

[5] M. Alzenad, A. El-Keyi, F. Lagum, and H. Yanikomeroglu, "3-D Placement of an Unmanned Aerial Vehicle Base Station (UAV-BS) for Energy-Efficient Maximal Coverage," *IEEE Wireless Communications Letters*, vol. 6, no. 4, pp. 434-437, Aug. 2017. Article (CrossRef Link)

[6] J. Cho and J. Kim, "Performance Comparison of Heuristic Algorithms for UAV Deployment with Low Power Consumption," in *Proc. of 2018 International Conference on Information and Communication Technology Convergence (ICTC)*, pp. 1067-1069, 2018. Article (CrossRef Link)

[7] R. I. Bor-Yaliniz, A. El-Keyi, and H. Yanikomeroglu, "Efficient 3-D placement of an aerial base station in next generation cellular networks," in *Proc. of 2016 IEEE International Conference on Communications (ICC)*, pp. 1-5, 2016. Article (CrossRef Link)

[8] Y. Zeng, R. Zhang and T. J. Lim, "Wireless communications with unmanned aerial vehicles: opportunities and challenges," *IEEE Communications Magazine*, vol. 54, no. 5, pp. 36-42, May. 2016. Article (CrossRef Link)

[9] M. Mozaffari, W. Saad, M. Bennis, and M. Debbah, "Efficient Deployment of Multiple Unmanned Aerial Vehicles for Optimal Wireless Coverage," *IEEE Communications Letters*, vol. 20, no. 8, pp. 1647-1650, Aug. 2016. Article (CrossRef Link)

[10] D. Orfanus, F. Eliassen, and E. P. de Freitas, "Self-organizing relay network supporting remotely deployed sensor nodes in military operations," in *Proc. of 2014 6th International Congress on Ultra Modern Telecommunications and Control Systems and Workshops (ICUMT)*, pp. 326-333, 2014. Article (CrossRef Link)

[11] H. Zhao, H. Wang, W. Wu, and J. Wei, "Deployment Algorithms for UAV Airborne Networks Toward On-Demand Coverage," *IEEE Journal on Selected Areas in Communications*, vol. 36, no. 9, pp. 2015-2031, Sept. 2018. Article (CrossRef Link)

[12] H. Wang, H. Zhao, W. Wu, J. Xiong, D. Ma, and J. Wei, "Deployment Algorithms of Flying Base Stations: 5G and Beyond With UAVs," *IEEE Internet of Things Journal*, vol. 6, no. 6, pp. 10009-10027, Dec. 2019. Article (CrossRef Link)

[13] X. Liu, Y. Liu, and Y. Chen, "Deployment and Movement for Multiple Aerial Base Stations by Reinforcement Learning," in *Proc. of 2018 IEEE Globecom Workshops (GC Wkshps)*, pp. 1-6, 2018. Article (CrossRef Link)
[14] K. Mitra, A. Zaslavsky, and C. Ahlund, "Context-aware QoE modelling, measurement, and prediction in mobile computing systems," *IEEE Trans. Mobile Computing.*, vol. 14, no. 5, pp. 920–936, May. 2015. Article (CrossRef Link)
[15] J. Cui, Y. Liu, Z. Ding, P. Fan, and A. Nallanathan, "QoE-Based Resource Allocation for Multi-Cell NOMA Networks," *IEEE Transactions on Wireless Communications*, vol. 17, no. 9, pp. 6160-6176, Sept. 2018. Article (CrossRef Link)
[16] A. M. Seid, G. O. Boateng, S. Anokye, T. Kwantwi, G. Sun and G. Liu, "Collaborative Computation Offloading and Resource Allocation in Multi-UAV-Assisted IoT Networks: A Deep Reinforcement Learning Approach," *IEEE Internet of Things Journal*, vol. 8, no. 15, pp. 12203-12218, 1 Aug.1, 2021. Article (CrossRef Link)
[17] J. S. Lee, Y. -S. Yoo, H. Choi, T. Kim, and J. K. Choi, "Group Connectivity-Based UAV Positioning and Data Slot Allocation for Tactical MANET," *IEEE Access*, vol. 8, pp. 220570-220584, 2020. Article (CrossRef Link)
[18] Y. Wang, C. Feng, T. Zhang, Y. Liu and A. Nallanathan, "QoE Based Network Deployment and Caching Placement for Cache-Enabling UAV Networks," in *Proc. of ICC 2020 - 2020 IEEE International Conference on Communications (ICC)*, pp. 1-6, 2020. Article (CrossRef Link)
[19] A. Al-Hourani, S. Kandeepan, and A. Jamalipour, "Modeling air-to-ground path loss for low altitude platforms in urban environments," in *Proc. of 2014 IEEE Global Communications Conference*, pp. 2898-2904, 2014. Article (CrossRef Link)
[20] M. Alzenad, A. El-Keyi, and H. Yanikomeroglu, "3-D Placement of an Unmanned Aerial Vehicle Base Station for Maximum Coverage of Users With Different QoS Requirements," *IEEE Wireless Communications Letters*, vol. 7, no. 1, pp. 38-41, Feb. 2018. Article (CrossRef Link)
[21] W. Liu, G. Niu, Q. Cao, M. Pun, and J. Chen, "3-D Placement of UAVs Based on SIR-Measured PSO Algorithm," in *Proc. of 2019 IEEE Globecom Workshops (GC Wkshps)*, pp. 1-6, 2019. Article (CrossRef Link)
[22] S. A. Hadiwardoyo et al., "optimizing UAV-to-Car Communications in 3D Environments Through Dynamic UAV Positioning," in *Proc. of 2019 IEEE/ACM 23rd International Symposium on Distributed Simulation and Real Time Applications (DS-RT)*, pp. 1-8, 2019. Article (CrossRef Link)
[23] H. J. Na and S. Yoo, "PSO-Based Dynamic UAV Positioning Algorithm for Sensing Information Acquisition in Wireless Sensor Networks," *IEEE Access*, vol. 7, pp. 77499-77513, 2019. Article (CrossRef Link)
[24] Q. Wang, A. Zhang, and L. Qi, "Three-dimensional path planning for UAV based on improved PSO algorithm," in *Proc. of The 26th Chinese Control and Decision Conference (2014 CCDC)*, pp. 3981-3985, 2014. Article (CrossRef Link)
[25] E. Wu, Y. Sun, J. Huang, C. Zhang, and Z. Li, "Multi UAV Cluster Control Method Based on Virtual Core in Improved Artificial Potential Field," *IEEE Access*, vol. 8, pp. 131647-131661, 2020. Article (CrossRef Link)
[26] UAV_Deployment Demo, Baidu, 2017. [Online]. Available: https://pan.baidu.com/s/1o7He78I

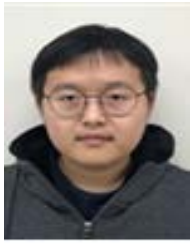

Young Jeon received his B.S. and M.Sc. degree in Information and Communications Engineering from Chungbuk national University, Republic of Korea, in 2020. He is currently working toward the Ph.D. degree at the Department of information and Communications Engineering, Chungbuk National University, Republic of Korea. His research areas include ad hoc network, time synchronization, and unmanned aerial vehicle.

Wonseok Lee received his B.S. and M.Sc. degree in Information and Communications Engineering from Chungbuk national University, Republic of Korea, in 2021. He is currently working toward the Ph.D. degree at the Department of information and Communications Engineering, Chungbuk National University, Republic of Korea. His research areas include unmanned aerial vehicles network and reinforcement learning.

Tran Manh Hoang received the B.S. degree in communication command from the Ministry of Defense, Telecommunications University, Nha Trang, Vietnam, in 2002, the B.Eng. degree in electrical engineering from Le Quy Don Technical University, Ha Noi, Vietnam, in 2006, the M.Eng. degree in electronics engineering from the Posts and Telecommunications Institute of Technology, Ho Chi Minh City, Vietnam, in 2013, and the Ph.D. degree from Le Quy Don Technical University in 2018. He is currently an Assistant Professor with Telecommunications University. His research interests include energy harvesting, non-orthogonal multiple access, and signal processing for wireless cooperative communications.

Taejoon Kim received his B.S. in Electronics Engineering from Yonsei University, Seoul, Republic of Korea, in 2003, and his PhD in Electrical Engineering from the Korea Advanced Institute of Science and Technology (KAIST), Daejeon, Republic of Korea, in 2011. He is currently a professor with the School of Information and Communication Engineering, Chungbuk National University, Chungju, Republic of Korea. From 2003 to 2005, he was a researcher with LG Electronics, Seoul, Republic of Korea. From 2011 to 2013, he was a senior researcher with Electronics and Telecommunications Research Institute (ETRI), Daejeon, Republic of Korea. His research areas include communication theory and analysis, optimization of wireless networks, reinforcement learning, and edge computing.